

Silver and mesoporous silica nanocomposites for the selective oxidation of benzyl alcohol

A
Dissertation submitted
In the partial fulfillment of the requirements for the degree of
M.Sc. (Chemistry)



Submitted by
Anjali Garg
(310402003)

Supervisor
Dr. Satnam Singh
Professor

School of Chemistry & Biochemistry
Thapar University, Patiala-147004
July 2016

Certificate

Acknowledgement

First of all, I owe my gratitude to the Head of the Department, **Dr. Bonamali Pal** for providing me an opportunity in the form of this dissertation to develop my interest in research.

In the same spirit, I would like to thank my Supervisor, **Dr. Satnam Singh** for their constructive guidance and constant support during the project. The work presented here could not have been accomplished without their patience and ever willingness to teach. They have taught me to be concise and correct in my approach from the formulation of ideas to the presentation of the results.

Special thanks to all the **Teaching Faculty** of the department for their cooperation and guidance.

I would also like to express my gratitude to **Ms. Shweta sareen** and **Mr. Roopchand Prajapat**, who never turned me down whenever I approached them for any kind of help. My heartfelt thanks to all the research scholars for their assistance.

I am grateful to **Thapar University & School of chemistry & biochemistry** for providing financial support and all necessary infrastructure and laboratory facilities to carry out the experimental work.

Words fail me to express my thanks to my family and friends who have always supported me and have been a source of strength and inspiration to me during the entire period of the work.

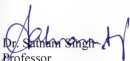
All these thanks are, however, only fraction of what is due to almighty for granting me an opportunity and strength to successfully accomplish this project.

Date: 15-7-18

Anjali Garg
Anjali Garg

Certificate

This is to certify that the dissertation entitled, "Silver and mesoporous silica nanocomposites for the selective oxidation of benzyl alcohol" being submitted by Ms. Anjali Garg in partial fulfillment of the requirements for the award of degree of Master of Science in Chemistry to the School of Chemistry and Biochemistry, Thapar University, Patiala, is a bonafide work carried out by her under my supervision. The contents of this dissertation have not been submitted for the award of any other degree or diploma.



Dr. Satish Singh
Professor
School of Chemistry & Biochemistry,
Thapar University, Patiala-147004

Countersigned by



Dr. Bonamali Pal
Professor & Head
School of Chemistry & Biochemistry,
Thapar University, Patiala-147004



Dr. S.S. Bhatia
Dean Academic Affairs
Thapar University, Patiala-147004

Candidate's Declaration

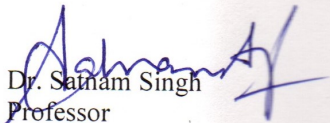
I hereby declare that the work being presented in the dissertation entitled "**Silver and mesoporous silica nanocomposites for the selective oxidation of benzyl alcohol**" in partial fulfillment of the requirements for the award of degree of Master of Science in Chemistry, and being submitted to School of Chemistry & Biochemistry, Thapar University, Patiala, is my own work during the period of January to July 2016, under the supervision of **Dr. Satnam Singh**. I have not submitted the contents embodied in this dissertation for the award of any other degree.


Patiala


Date: 15/7/16


Anjali Garg

This is to certify that the **statement** made by the candidate is correct and true to the best of our knowledge.


Dr. Satnam Singh
Professor
School of Chemistry & Biochemistry,
Thapar University, Patiala-147004


Dr. Bonamali Pal
Professor & Head
School of Chemistry & Biochemistry,
Thapar University, Patiala-147004


Dr. S.S. Bhatia
Dean Academic Affairs
Thapar University, Patiala-147004

Abstract

Silver nanoparticles loaded mesoporous SBA-15 nanocomposites prepared by direct synthesis and incipient wetness impregnation methods were evaluated as catalysts for the selective oxidation of benzyl alcohol to benzaldehyde. The prepared nano composites were characterized by Powder XRD, TEM, TGA, BET, FTIR and DRS techniques. Powder XRD confirmed the existence of metallic Ag nano particles in the mesoporous sieves. TEM images showed uniform distribution of Ag nano particles as dark nanostructures in- as well as on- the surface of SBA-15. The surface area of bare SBA-15 significantly changed with the introduction of metal within the silica host. Thus, the physiochemical and catalytic parameters of the synthesized nanocomposites were found to be greatly influenced by the method used for the preparation of the nanocomposites. Moreover, among the different nanocomposites, Ag/AP-SBA-15(T) nanocomposites exhibited the highest catalytic activity for the selective oxidation of benzyl alcohol to benzaldehyde (87 %) and benzyl benzoate in IPA/H₂O (1:1) resulting in complete oxidation of the compound.

List of Figures

Figure 1 - Solid state UV-Vis absorbance spectra of Ag incorporated SBA-15 nanocomposites

Figure 2 – FTIR spectra of SBA-15 and different Ag loaded SBA-15 catalysts

Figure 3 a – Low angle XRD pattern

Figure 3 b – wide angle XRD pattern

Figure 4-TEM images of (a) Ag/SBA-15, (b) Ag/AP-SBA-15(O) and (c) Ag/AP-SBA-15(T) nanocomposites

Figure 5 - SEM and EDS spectra of Ag/AP-SBA-15(T) nanocomposites.

Figure 6 - TGA curve of bare SBA-15 and different Ag loaded SBA-15 catalysts

Figure 7 - Product distribution of oxidation of benzyl alcohol (2 mM) to benzaldehyde and benzyl benzoate respectively by bare SBA-15 and different Ag loaded SBA-15 catalysts

Figure 8 -GC-MS of reaction mixture of Ag/AP-SBA-15(T) nanocomposites at 3 h of reaction

List of abbreviations and symbols

°C – Degree Celsius
% - Percent
g- grams
mg- milligram
M – Molarity
kg- kilograms
L – litres
Min – minutes
nm- nanometre
GC-MS – Gas Chromatography spectrometry
SEM – Scanning electron microscope
TEM – transmission electron microscope
FT-IR – Fourier transform infra red spectroscopy
SBA-15 – Santa Barbara Amorphous type material
BET – Brunauer – Emmett- Teller
Conc. – concentration

List of contents

Content	Page number
1. Introduction	1 -2
2. Literature review	3 – 8
3. Objectives	
4. Experimental, Materials and methodology	8 - 8
5. Results and discussion	8 - 18
6. Conclusion	18
7. References	19 - 21

1. Introduction

In the recent years, porous materials have been extensively employed because of their highly ordered shape, size, selectivity, stability and catalytic activity leading to a wide variety of applications in the nanomaterial or applied science[1, 2]. Usually, these are divided into three categories, namely microporous, mesoporous and macroporous based on the difference in their respective shapes, sizes of their framework network and catalytic activity. Among them, mesoporous materials are the porous materials that have a pore diameter in the range of 2-50 nm. They are amorphous, made up of silica frame-work having high surface area, larger pore-size, ordered arrays of nano-channels, higher hydrothermal stability with potential applications in separation, catalysis, adsorption and synthesis[3].

Initially, Mobil Oil Research & Development [4], scientists synthesized a wide variety of the mesoporous materials by using cationic surfactants to assemble silicate anions from solution thus forming the mesoporous molecular sieves. Moreover, in 1998 Zhao et al.[5] embarked a new revolution in material chemistry by discovering SBA-15 (Santa Barbara Amorphous) with increased thermal and hydrothermal stability in comparison to the other materials with a broad range of pore-size (4.6-30 nm) and pore wall thickness (3.1-6.4 nm) by using poly(ethyleneoxide) poly(propyleneoxide) poly(ethyleneoxide) triblock copolymer ($\text{EO}_x\text{PO}_y\text{EO}_x$) as a template[6]. Although SBA-15 exhibited many advantages, yet it was found to be an inert catalytic support but when metal was incorporated into it by impregnation or other techniques, these materials acted as efficient heterogeneous catalysts for a variety of industrially important reactions [7-11]. Furthermore, it has also been established that the physical and structural properties of the prepared metal incorporated SBA-15 nanocomposites are strongly related to their preparation conditions, nature of metal, calcinations temperature etc. So, different techniques [12-15] were employed for the synthesis of metal loaded mesoporous nanocomposites. However, the simplest method is one-pot method involving the addition of metal precursor during the synthesis process leading to the incorporation of metal into the framework. Being a direct method, it controls the pore size, pore structure and the amount of metal incorporated within the support and thus, has been used for the incorporation of different metals viz., Al, Co, Ag and Pt on the mesoporous support[16-18]. Piquemal et al. [12] showed

one-step formation of Ag nanowires in mesoporous SBA-15 using polyol process. Tian et al. [19] prepared SBA-15 supported Ag NPs by in-situ reduction method using hexamethylenetetramine as a mild reducing agent (HMTA). The second method, incipient wetness impregnation [20] involved preparation of supported catalysts when the metal salt solution is added to the preformed support in an amount to fill the exact pore volume and then the material is dried and calcined. For metal incorporation, the support was also activated by functionalization of its surface by various organic groups like amines or thiols or -COOH resulting in confinement of metal in the highly dispersed form in the mesochannels of the host [21-23]. Reports based on the incorporation of different transition metals on SBA-15 by the post-modified (two-pot) method are being discussed. Huang et al. [24] studied the effect of surface properties of SBA-15 on confined Ag NPs by double solvent technique and observed that the morphology as well as the dispersion of the incorporated Ag NPs can be easily controlled by adjusting the surface properties of SBA-15. Chimentao et al. [25] prepared Ag NPs incorporated SBA-15 composites by a two-pot method for the reduction of p-nitrophenol to p-aminophenol. Zhang et al. [26] prepared SBA-15 supported Ag NPs by impregnation method for catalyzing CO oxidation. Lin et al. [27] prepared Ag NPs confined in mesoporous SBA-15 and used it as a sensor for the detection of H₂O₂. Fuku et al. [28] reported the preparation of Ag/SBA-15 composites by microwave heating for evaluating their catalytic activity for the production of H₂ from NH₃BH₃. Zhu et al. [29] reported the incorporation of Ag NPs in mesoporous SBA-15 by two-pot method for the liquid phase separation of aromatic hydrocarbons. Szegedi et al. [30] synthesized Ag NPs in SBA-15 by using pulsed laser ablation and found that the prepared composites showed high catalytic activity and stability for the oxidation of toluene. Although, a number of reports have been dedicated for the preparation of Ag/SBA-15 nanocomposites by different synthetic methods, yet it has been observed that there are few reports on the comparison of changes in physiochemical properties of prepared Ag loaded SBA-15 composites, synthesized by different methods viz., in terms of their size, dispersion density of metal NPs and evaluation of the catalytic activity for different oxidation reactions particularly the selective oxidation of benzyl alcohol to benzaldehyde.

2. Literature review

Synthesis, characterization and application of porous materials have strongly promoted its broad use as catalysts, adsorbents and sensors[31]. Mesoporous materials have been the centre of scientific interest because of their uniform structures, high surface areas, and tunable pore sizes. These properties made them ideal templates to control the shape and size of incorporated metal for the preparation of metal NPs. These NPs can be synthesized through various pathways using different types of surfactants (used as the template) and inorganic species. These pathways has been classified depending upon the interaction between the surfactant and the inorganic framework. Huo et al. [32] proposed mainly four different reaction pathways for synthesis of mesoporous materials.

1. S⁺I⁻ route: In this route, (S⁺) is used as a cationic surfactant and (I⁻) as an anionic inorganic species. It involves the co-condensation of anionic with a cationic surfactant to form assembled ion pair (S⁺I⁻). It is basically used for the synthesis of M41S materials [4].

2. S⁻I⁺ route: In this route, the anionic surfactant (S⁻) interacted with cationic inorganic species (I⁺), and is used to direct the self-assembly of cationic inorganic species (I⁺) via (S⁻) ion pairs.

3. S⁺XI⁺ route: In this route, the surfactant and the inorganic species are cationic in nature and interact with the negatively charged (X⁻ = Cl⁻, Br⁻ halogens) ions.

4. S⁻M⁺I⁻ route: This route involves the interaction between anionic surfactant and inorganic species and the positively charged M (metal = Na⁺, K⁺) species.

5. S⁰I⁰ route: This route has been proposed by Tanev et al. [33] that used neutral primary amine surfactant and neutral inorganic species as precursors for the synthesis of mesoporous materials. The route 3 and 4 involved counter ion (X⁻ or M⁺) mediated assemblies of surfactant and inorganic species of a similar charge. These counter ion-mediated routes afforded assembled solution species of the type S⁺XI⁺ or S⁻M⁺I⁻.

Moreover, though mesoporous materials were synthesized by different routes as proposed above yet they were completely inert when used in catalysis. For the preparation of heterogeneous catalyst, immobilization of metal on mesoporous materials was a useful process as it was observed that the metal NPs incorporated inside the mesoporous materials were found to be in a

highly dispersed and stabilized form and resulted in their high catalytic efficiency. Moreover, it also gave an insight into the changes associated with the physiochemical properties of different metal NPs confined in various molecular sieves. Primarily, transition metals have been incorporated within the mesoporous support. Hojipour et al.[34] prepared the Platinum supported SBA-15 by impregnated method or by an ultrasonic method using a different concentration of Platinum salt (0.005%) for the hydrogenation and dehydrogenation of cyclohexene. Tao et al. [35] synthesized a series of Ni/SBA-15 materials by using impregnation method for the production of synthetic natural gas. Rudolf et al.[36] synthesized Cu NPs supported on the polyether functionalized mesoporous silica by an evaporation induced self-assembly method and used them for the hydrogenation of cinnamaldehyde. Tu et al.[37] reported the preparation of Cu NPs incorporated SBA-15 composites by a two-pot method for the CO oxidation. Vinoba et al.[38]reported the synthesis of Ag NPs incorporated amine grafted SBA-15 composites by grafting method for the electro catalytic reduction of H_2O_2 . Du et al.[39] reported the formation of Vanadium oxide incorporated mesoporous silica nanocomposites by controlled grafting method for the oxidation of methanol. Besides, the above reported reactions there has been an exponential increase in the number of publications involving mesoporous catalysts for alcohol oxidation.

Oxidation of alcohols to carbonyl compounds has established itself as an important application in the chemical process industry because carbonyl compounds such as aldehydes, ketones form an important component in the synthesis of many organic compounds, vitamins, complex ligands as well as medicine[40-42]. Among various aldehydes, benzaldehyde is a valuable chemical substance and has widespread applications in chemical industries. As a result, various papers are dedicated for the oxidation of benzyl alcohol to benzaldehyde respectively. Li et al. [43] reported photo catalytic oxidation of benzyl alcohol to benzaldehyde by single crystalline Rutile TiO_2 nano-rods using visible light. Choudhary et al. [44] prepared transition metal containing mixed oxides for oxidation of benzyl alcohol using tertiarybutylhydroperoxide (TBHP) as an oxidant. Similarly, Mistri et al. [45] and Behra et al. [46] prepared Cu loaded $LaFeO_3$ perovskites and VPO (vanadium phosphate oxide) heterogeneous catalysts respectively for benzyl alcohol oxidation using TBHP as an oxidant. Since the common methods of alcohol oxidation used toxic, corrosive, expensive solvents and oxidants, strong mineral acids, reagents of transition metal complexes such as chromium and cobalt, setting up severe conditions like high pressure or

temperature [47]. Many of them experienced the disadvantages like lack of availability, difficulty in work-up, long reaction time, cost of metal catalysts, as well as toxicity and high cost of the reagents. Thus, moderate, more selective eco-friendly reagents are a necessity. So, Li et al. [43] studied the aerobic oxidation of benzyl alcohol using Pd/SBA-15 catalysts under solvent-free conditions in the absence of any additives. Choudhary et al. [44] prepared the gold NPs supported on various alkaline earth metal oxides (MgO, CaO, BaO and SrO), (Al_2O_3 , Ga_2O_3 , In_2O_3 and Tl_2O_3) and transition metals oxides (TiO_2 , Cr_2O_3 , MnO_2) respectively by deposition precipitation and by homogeneous deposition precipitation methods for the solvent free oxidation of benzyl alcohol to benzaldehyde. Alabbad et al. [48] reported the synthesis of silver and gold NPs supported manganese oxide nanocomposites by co-precipitation method for the oxidation of benzyl alcohol into benzaldehyde using molecular oxygen as a source of oxygen. Geng et al. [49] prepared highly dispersed FeO supported mesoporous carbon (CMK-3) nanocomposites by one -pot evaporation method for the oxidation of benzyl alcohol to benzaldehyde by using air as an oxidant. Over the past few years, importance of hydrogen peroxide (H_2O_2) and its derivatives as oxidizing agents has also developed very much. From an environmental effect, in comparison to other oxidizing agents, H_2O_2 is the most interesting one, as it produces water as the only byproduct in this process. Moreover, it can be stored safely, easily operated as well as transported, comparatively cheap and widely available in the market. Adam et al. [50] reported the formation of rice husk silica catalyst incorporated with 10% wt. of Vanadium by a sol-gel synthetic route for the liquid phase oxidation of acetophenone into benzoic acid and benzyl formic acid. Jia et al. [51] reported the synthesis of selective oxidation of benzyl alcohol to benzaldehyde with H_2O_2 over alkali-treated ZSM-5 zeolite catalysts. The results showed that though the catalyst was very stable yet the conversion of benzyl alcohol and the selectivity to benzaldehyde were about 53% and about 86% respectively.

It is thus established that different methods were used for catalyzing oxidation of benzyl alcohol; however, there have been few reports using noble metal based mesoporous catalysts exhibiting high selectivity for oxidation of benzyl alcohol to benzaldehyde. In this context, the present work describes the preparation of highly active and dispersed Ag NPs incorporated SBA-15 catalysts prepared by an in-situ and post modified method (without the use of any toxic or expensive reducing agents) for catalyzing the selective oxidation of benzyl alcohol using

hydrogen peroxide as the oxidant. Moreover, comparison of the changes in the physiochemical and catalytic parameters of the prepared nanocomposites have also been described.

3. Objectives

3.1 To prepare mesoporous SBA-15.

3.2 To prepare Ag incorporated mesoporous SBA-15 nanocomposites by different methods (viz., in-situ and post modification).

3.3 To study the comparative catalytic activity and physiochemical properties of prepared nanocomposites for oxidation of benzyl alcohol.

4. Experimental

4.1 Materials: Pluronic(P123), tetraethylorthosilicate (TEOS, 99%), 3-aminopropyltrimethoxysilane(APTMS, 97.0%), silver nitrate(AgNO_3 , 99.0 %), benzyl alcohol(B.A.), benzaldehyde (B.D.), benzoic Acid, benzyl benzoate(B.B.A.), isopropyl alcohol (IPA), hydrogen peroxide (H_2O_2 , 30 wt.%), hydrochloric Acid (HCl, 37 %), methanol and ethanol. De-ionized water with ultra-pure filtration system (Milli-Q, Millipore) was used throughout the experiments.

4.2 Catalyst Preparation:

4.2.1 Preparation of Ag incorporated SBA-15 nanocomposites by two-pot (post-modification) method

a) Preparation of SBA-15:

Mesoporous SBA-15 was prepared by reported method [5] by mixing 2g of Pluronic(P123) in 60ml of 2M HCl solution under stirring for 3h at room temperature till a clear solution was obtained. Then 5 ml of TEOS was added to the above solution under stirring for 24 h, followed by autoclaving for 48 h at 100°C . It was filtered, dried overnight at 80°C and finally calcined at 550°C for 8 h at a heating rate of $1^\circ\text{C}/\text{min}$.

b) Surface modification with APTMS

The surface modification of SBA-15 with APTMS was done by adding 100 ml of 1 wt. % of ethanolic solution of APTMS to 2g of pure SBA-15 under stirring for 3 h. Finally, it was filtered, dried and used as AP-SBA-15.

c) Preparation of Ag incorporated SBA-15 nanocomposites

For the preparation of Ag incorporated SBA-15 nanocomposites by two-pot method, 500 mg of AP-SBA-15 was impregnated with 46.3 ml of 2 mM aqueous solution of AgNO_3 , stirred for 3 h, filtered, dried overnight at 60°C and calcined at 350°C for 2 h resulting in the formation of dark grey powdered material designated as Ag/AP-SBA-15 (T). For comparison and to evaluate the role of APTMS, bare SBA-15 was directly impregnated with a given amount of 2 mM AgNO_3 solution under stirring for 3 h, filtered, dried at 60°C and finally calcined at 350°C for 2 h and the sample was designated as Ag/SBA-15.

4.2.2 Preparation of Ag incorporated SBA-15 nanocomposites by one-pot (in-situ) method

For the synthesis of Ag loaded SBA-15 nanocomposites by in-situ method. 2 g of Pluronic was dissolved in 60 ml of 2 M HCl solution until a clear solution was obtained, followed by the addition of 46.3 ml of 2 mM AgNO_3 solution and an appropriate amount of 1 wt. % APTMS solution, stirred for another 2 h at 35°C . Followed further by the addition of 4.5 ml of TEOS under stirring for 24 h. The contents of the beaker were then autoclaved for 48 h, filtered, dried at 60°C and finally calcined at 550°C for 8 h leading to the formation of light grey Ag/AP-SBA-15(O).

4.2.3 Catalyst characterization

Distinct characterization techniques like TGA, FT-IR, EDX, SEM, Powder XRD, TEM, BET and Solid-state UV-vis absorbance spectra were used to characterize the synthesized materials. Solid-state UV-visible absorption spectra were obtained within the range of 400-800 nm by using Analytikjena Specord 205 spectrophotometer. TGA-50 Shimadzu Thermo gravimetric analyzer was used for thermal analyses within the temperature range of $100\text{-}800^\circ\text{C}$ at a heating

rate of 1°C/min under nitrogen and ambient atmospheric pressure. IR spectra were recorded on Cary 660 series Agilent FTIR spectrometer within the range of 400-4000 cm⁻¹ using KBr pellet method. Transmission electron images were obtained using Hitachi (H-7500) operating at 120 kW. FEI Tecnai F20 microscope was used to obtain the SEM and EDX images operated at 200kV. Powder X-ray diffraction (XRD) patterns were recorded on analytical Expert Pro X-Ray diffractometer utilizing Cu-K α radiation ($\lambda=1.54 \text{ \AA}$) within the 2θ range of 0.5-5° and 10-80°. The crystallite size of the samples was calculated by using Scherrer equation, $D = k\lambda/\beta\cos \theta$ where D is the average crystallite size, λ is the X-ray wavelength, k is a constant, θ is the diffraction angle and β is full width at half maxima of the diffraction line. Surface area measurements were determined by pre treatment of 20 mg of all the samples at the 150°C for 2 h using BET surface area analyzer (Smartsorb 92/93).

4.2.4 Catalytic activity

Catalytic activity and stability of prepared Ag loaded SBA-15 catalysts was evaluated for oxidation of benzyl alcohol by adding catalyst (10 mg) to a solution of substrate (10 ml, 2 mM) in aqueous IPA (50 vol. %) and H₂O₂ (6 μ l) under constant stirring at 90°C, appropriately. The analysis of the products was done on HPLC (Agilent 1120 compact LC using C-18 column) at wavelength of 254 nm using MeOH: H₂O (70:30) as a mobile phase with a flow rate of 1 ml/min. Moreover, GC-2010 and GCMS QP 2010 plus with RTX-5SIL-MS column (30 \times 0.25 \times 0.25mm) were used to determine the formation of products and intermediates (if any) formed during the course of reaction. Helium was used as a carrier gas with a flow rate of 1ml min⁻¹ at 60°C to 290°C @ 60°C min⁻¹ rise of temperature.

5. Results & Discussion

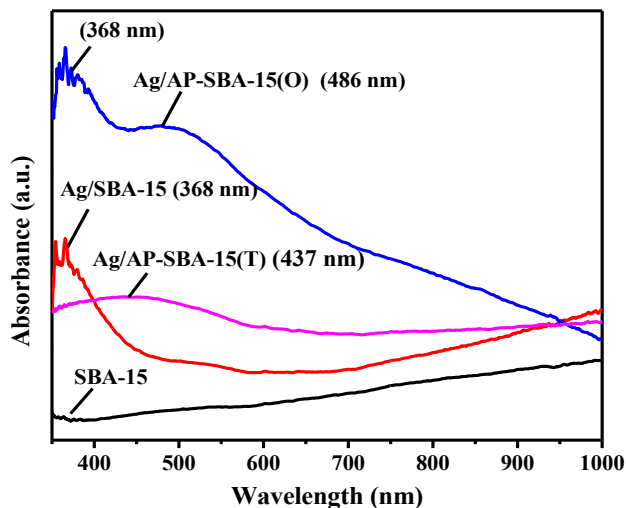


Fig.1 Solid state UV-Vis absorbance spectra of Ag incorporated SBA-15 nanocomposites

5.1 Solid-state UV-visible studies

The solid- state UV-visible absorption spectra of Ag incorporated SBA-15 composites (Fig. 1) represented bands at 368 nm, 437 nm, 368 nm and 486 nm wavelength respectively while no band was observed for bare SBA-15. Generally, presence of a band at 437 nm

is characteristic to the formation of Ag NPs within the mesoporous SBA-15[52]. However, for Ag/SBA-15 composites appearance of a band at 368 nm corresponds to the quadruple plasm on resonance [24]. In contrast, two bands were observed for Ag/AP-SBA-15(O) nanocomposites that attributed to the quadruple and dipole plasm on resonance respectively [53]. Further it indicated the probability of aggregation of some of the Ag NPs on the surface of the mesoporous support [54]. Moreover, for Ag/AP-SBA-15(T) nanocomposites, presence of a single band at 437 nm signified the presence of spherical Ag NPs within the mesoporous sieves [24]. It can thus be concluded that dispersion of the embedded metal NPs is greatly influenced by the different methods of preparation.

5.2 FT-IR studies

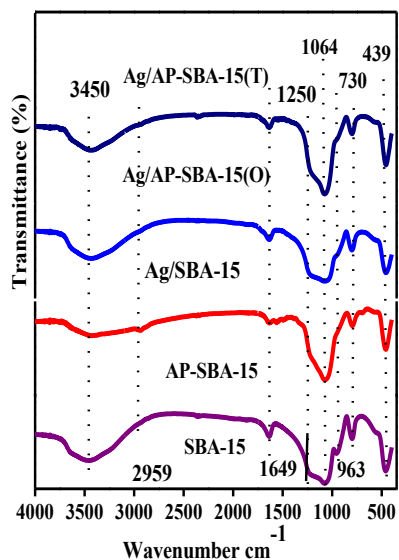


Fig. 2 FTIR spectra of SBA-15 and different Ag loaded SBA-15 catalysts.

FT-IR spectra (Fig. 2) of SBA-15 exhibited characteristic absorption bands at 3450 cm^{-1} and 1649 cm^{-1} due to the bond stretching and bending vibrations of the silanol groups [55]. The strong absorbance band at 1064 cm^{-1} can be assigned to the asymmetric stretching (AS) modes of Si-O-Si vibrational mode [56]. Moreover, the AS vibrational mode consisted of two major components, one in phase motion of two adjacent oxygen atoms with respect to the central silicon atom (AS1) and the other out-of-phase motion of the two adjacent oxygen atoms with respect to the central silicon atom (AS2). In addition, each AS vibration mode is associated with transverse-optic (TO) and longitudinal-optic (LO) vibration modes. The bands at about 1064 and 1250 cm^{-1} are due to TO vibrational mode of AS1 stretching of Si-O-Si bond and LO vibrational mode of AS1 stretching of Si-O-Si bond, respectively. LO-TO pair bands of AS2 mode at 1188 cm^{-1} overlap with AS1 pair, resulting in a broad absorbance band at $1064\text{-}1324\text{ cm}^{-1}$ [56]. Another band at about 963 cm^{-1} can be assigned to overlapped vibration

FT-IR spectra (Fig. 2) of SBA-15 exhibited characteristic absorption bands at 3450 cm^{-1} and 1649 cm^{-1} due to the bond stretching and bending vibrations of the silanol groups [55]. The strong absorbance band at 1064 cm^{-1} can be assigned to the asymmetric stretching (AS) modes of Si-O-Si vibrational mode [56]. Moreover, the AS vibrational mode consisted of two major components, one in phase motion of two adjacent oxygen atoms with respect to the central silicon atom (AS1) and the other out-of-phase motion of the two adjacent oxygen atoms with respect to the central silicon atom (AS2). In addition, each AS vibration mode is associated with transverse-optic (TO) and longitudinal-optic (LO) vibration modes. The bands at about 1064 and 1250 cm^{-1} are due to TO vibrational mode of AS1 stretching of Si-O-Si bond and LO vibrational mode of AS1 stretching of Si-O-Si bond, respectively. LO-TO pair bands of AS2 mode at 1188 cm^{-1} overlap with AS1 pair, resulting in a broad absorbance band at $1064\text{-}1324\text{ cm}^{-1}$ [56]. Another band at about 963 cm^{-1} can be assigned to overlapped vibration

modes of unreacted SiO₂ and Si-OH stretching vibrations. The absorption band at about 730 cm⁻¹ in the lower-frequency region is related to the symmetric stretching mode of Si-O-Si bonds. Absorbance band at 439 cm⁻¹ confirmed the formation of pore wall of mesoporous silica (SBA-15) due to the rocking, bending and stretching of inter-tetrahedral oxygen atoms in the SiO₂ structure [57]. Furthermore, the band observed at 1649 cm⁻¹ is attributed to the amine group while the band at 2959 cm⁻¹ indicated the presence of alkane group (-CH₃). Similar type of spectra as that of SBA-15 were obtained for Ag loaded SBA-15 composites prepared by different methods that indicate the structural integrity of SBA-15 was maintained even after Ag incorporation and surface functionalization.

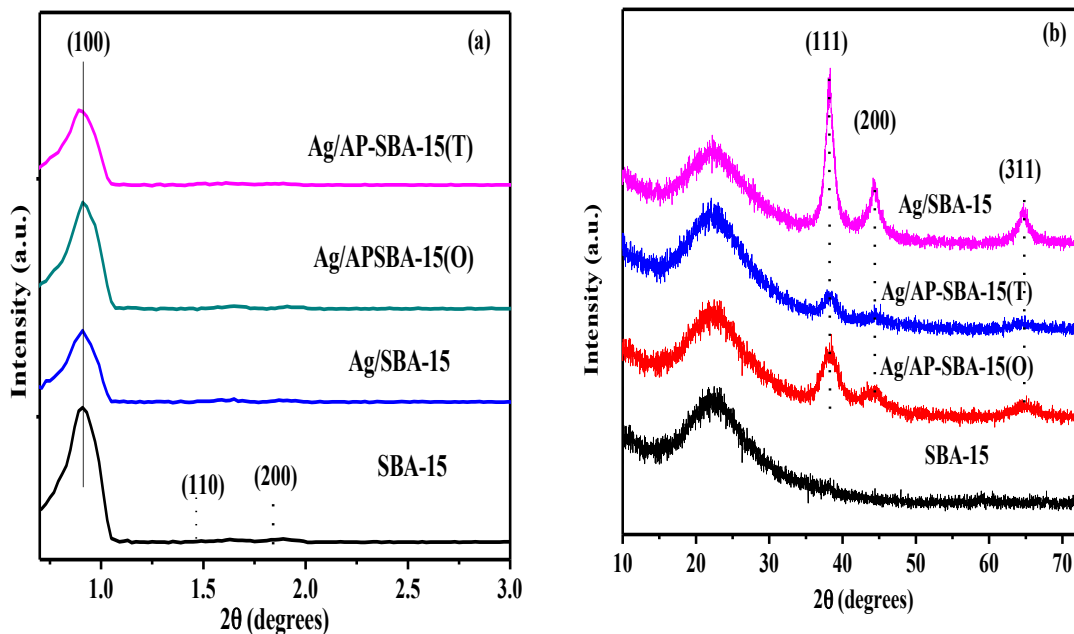
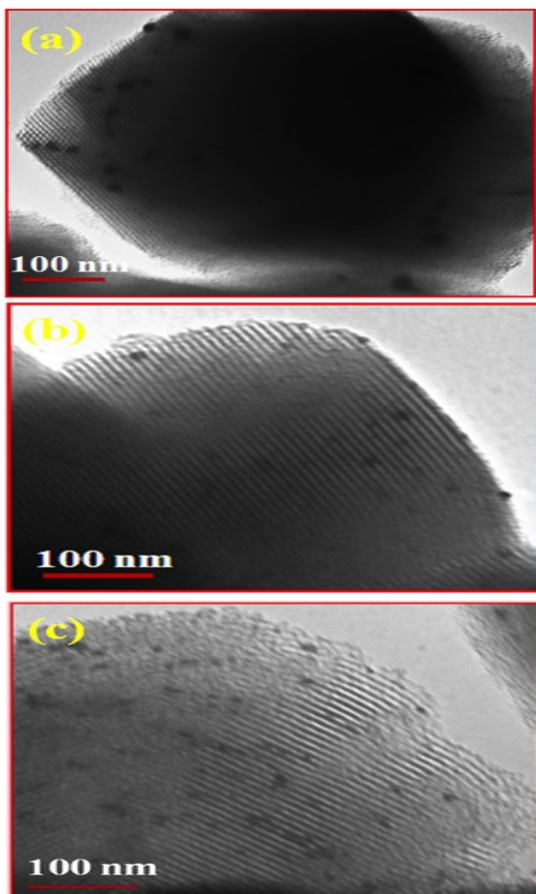


Fig. 3(a) Low angle and (b) wide angle XRD patterns of bare SBA-15 and different Ag loaded SBA-15 catalysts.

Fig. 4 TEM images of (a) Ag/SBA-15, (b) Ag/AP-SBA-15(O) and (c) Ag/AP-SBA-15(T) nanocomposites.



5.3 Powder XRD studies Low angle XRD pattern (Fig. 3a) of SBA-15 showed fine diffraction peaks at 1° , 1.5° and 1.8° corresponding to 100, 110 and 200 planes of the 2D hexagonal structure [51] of p6mm symmetry characteristic of mesoporous materials. Moreover, analogous XRD spectra observed for different Ag loaded SBA-15 composites further determined the existence of long range mesopore ordering and textural uniformity of SBA-15 by using different synthesis techniques. However, for different Ag incorporated SBA-15 composites a decrease in the intensity of 110 and 200 peaks was noticed because of pore filling effect [51] due to incorporation of Ag nanospecies within the silica host resulting, in the decrease in electron density between the mesochannels of the silica moiety. Moreover, for Ag/AP-SBA-

15(T), the peak corresponding to (100) plane shifted to lower 2θ value (from 1.00 to 0.97) indicating an increase in structural parameters viz., lattice spacing's and unit cell parameters (a_0) [51] (Table 1). The shuffling of the (100) peak signified the existence of Ag NPs within the mesopores [51] leading to the feeble disordering of the pore channels. Moreover, no shifting of peaks were observed for Ag/SBA-15 and Ag/AP-SBA-15(O) composites. This further illustrated different means of association of Ag NPs in and on the surface of a mesoporous moiety structure. Wide angle XRD pattern (Fig. 3b) of Ag loaded SBA-15 nanocomposites exhibited a band at 22° corresponding to amorphous silica walls of SBA-15 [16]. All the prepared nanocomposites exhibited a characteristic diffraction peaks at 38.3° , 44.3° and 77.5° respectively, illustrating the presence of metallic, Ag within the mesoporous sieves (JCPDS: 04-0783). Moreover, the average particle size as calculated from Scherrer equation was found to vary from ~ 30 nm, ~ 20 nm and ~ 8 nm for Ag/SBA-15, Ag//AP-SBA-15(O) and Ag/AP-SBA-15(T) respectively.

5.4 TEM

TEM images (Fig. 4a) of Ag/SBA-15 depicted large aggregates of irregularly shaped dark Ag NPs (size ~ 30 - 40 nm) scattered on the outer surface of the comparatively light mesoporous SBA-15 host. However, for Ag/AP-SBA-15(O), larger spherical Ag NPs (~ 15 nm) were seen evenly dispersed in the mesochannels of the host while a small amount of Ag NPs can also be seen near the entrance of the pore channels (Fig. 4b). In contrast, for Ag/AP-SBA-15(T) nanocomposites showed the presence of comparatively smaller Ag NPs (~ 8 - 10 nm) evenly dispersed throughout the mesoporous matrix (Fig. 4c). This indicated that the two-pot method helps in the formation of smaller Ag NPs besides leading to their efficient dispersal throughout the SBA-15 matrix. Moreover, it was observed that the Ag NPs were present entirely within the host channels. These results are in consonance with the wide angle XRD studies.

5.5 SEM and EDS

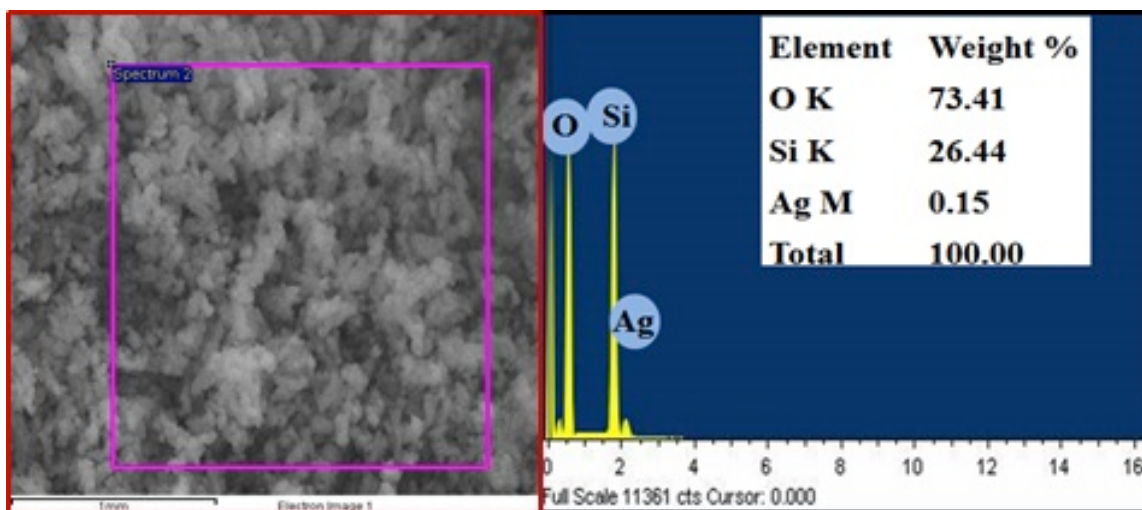


Fig. 5 SEM and EDS spectra of Ag/AP-SBA-15 (T) nano composites.

SEM image (Fig. 5) confirmed the existence of the rod shaped 2D hexagonal structure of SBA-15. Moreover, when the Ag was loaded, well-dispersed metal species were observed on the surface of SBA-15 [50]. The corresponding EDX spectra further evidenced the presence of Ag nanospecies within mesoporous host (Ag ~ 0.15 wt. %) respectively [50].

5.6 BET

Surface area studies demonstrated a decrease in the BET surface area of bare SBA-15 (560 m²/g) with Ag loading (Table 1). The surface area of Ag/SBA-15, Ag/AP-SBA-15(O) and Ag/AP-SBA-15(T) were found to be 594 m²/g, 538 m²/g and 485 m²/g, respectively. The probable decrease in the surface area of Ag loaded SBA-15 nanocomposites prepared by two pot method can be attributed to the presence of uniformly distributed smaller Ag NPs in the SBA-15 matrix. Moreover, it also suggests that Ag has incorporated within the host mesochannels. However, in contrast, the higher surface area (more than bare SBA-15) observed for Ag/SBA-15, Ag/AP-SBA-15(O) can be ascribed to the occurrence of the large Ag aggregates (for Ag/SBA-15) and Ag NPs on the surface of the silica host besides, present within the mesopores. These results are in accordance with the TEM and low angle XRD studies, respectively.

Table1 Physiochemical parameters for bare SBA-15 and different Ag loaded SBA-15 nanocomposites

Sample	d-spacing d_{100} (nm)	Unit cell parameter a_0 (nm) ^a	wall thickness d_w (nm) ^b	Surface area (m ² /g)
SBA-15	8.79	10.15	1.36	560
Ag/SBA-15	8.89	10.26	1.37	594
Ag/AP-SBA-15(O)	8.91	10.28	1.37	538
Ag/AP-SBA-15(T)	9.08	10.48	1.40	485

^a $a_0 = 2/3^{1/2}d_{100}$, ^b $d_w = a_0 - d_{100}$

5.7 Thermo gravimetric analysis

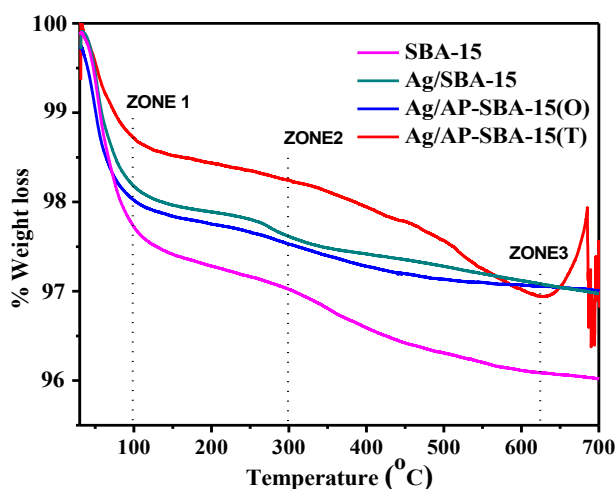


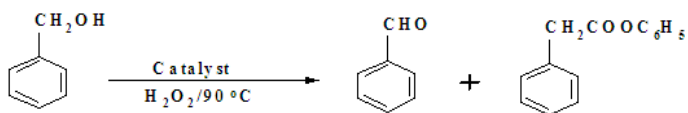
Fig. 6 TGA curve of bare SBA-15 and different Ag loaded SBA-15 catalysts.

The TGA spectra of SBA-15 and Ag loaded SBA-15 catalysts in (Fig. 6) exhibited degradation in three different wt. loss zones. The first wt. loss zone at 100 °C (constituting ~2.2 % for SBA-15, ~1.3% for Ag/AP-SBA-15 (T), ~1.9% for Ag/AP-SBA-15(O) and ~1.7 % Ag/SBA-15), is linked with the loss of physically adsorbed water molecules in silica channels and coordinated to Ag complexes. The second wt. loss (~0.5 % for SBA-15, ~0.3% Ag/AP-SBA-15(O), ~0.4 % for

Ag/SBA-15 and ~0.4 % Ag/AP-SBA-15(T) between 100 °C and 300 °C may be associated with the decomposition of remaining surfactant (if any) [58]. The third wt. loss zone (~1 % for SBA-15, ~0.3% Ag/AP-SBA-15(O) and ~1.2 % Ag/AP-SBA-15(T) between 300 °C and 650°C is ascribed to the decomposition of the amino propyl groups. However, above 670 °C a negligible wt. loss of ~0.1 % for SBA-15 and Ag loaded SBA-15 nanocomposites is related to the combustion of remaining carbon species and de-hydroxylation of Si-OH groups [59]. TGA studies supported the fact the prepared materials were found to be hydrothermally stable [60] and could be used as catalysts for reactions taking place at high temperature.

5.8 Catalytic activity

The catalytic performance of the prepared nanocomposites was evaluated for the oxidation of alcohols viz., oxidation of benzyl alcohol as a model reaction using H₂O₂ as a green oxidant.



Scheme 1 Selective oxidation of benzyl alcohol

Moreover, the conversion and selectivity of the products obtained was found to be greatly influenced by the synthesis methods that

indirectly controls the size, dispersion as well as amount of metal NPs present within as well as

on the surface of mesoporous SBA-15. For the control experiment, less than 1 % conversion of benzyl alcohol was observed with bare SBA-15, which signified that metal nano-species present within the sieves were the active sites for the reaction. It was found that among the different catalysts, Ag/AP-SBA-15(T) showed the highest catalytic activity with 100 % conversion and 87 % selectivity for benzaldehyde in 6 h of reaction (Fig. 7) quite comparable with the published reports [61]. Benzaldehyde was formed as the major product with the small amount of benzyl benzoate as the only by-product, which is also confirmed by the GC-MS analysis respectively (Fig. 8). Moreover, benzoic acid is not observed as the reaction product which is due to the fact that as soon as the benzoic acid is formed, it instantaneously reacts with the benzyl alcohol resulting in the formation of benzyl benzoate[46]. The order of the catalytic activity is: Ag/SBA-15<Ag/AP-SBA-15(O)<Ag/AP-SBA-15(T) respectively. The high catalytic activity of the Ag/AP-SBA-15(T) nanocomposites can be attributed to the increased dispersion of smaller Ag NPs that leads to the formation of increased number of active sites in the channels of SBA-15.

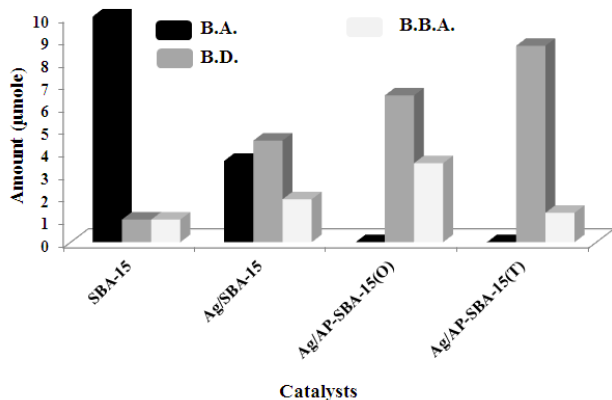


Fig. 7 Product distribution of oxidation of benzyl alcohol (2 mM) to benzaldehyde and benzyl benzoate respectively by bare SBA-15 and different Ag loaded SBA-15 catalysts.

As a result, more number of substrate molecules resulting in a greater catalytic efficiency will easily access greater number of active sites. Among the various catalysts, lowest conversion was observed in case of Ag/SBA-15 probably due to the formation of larger Ag aggregates that block the mesochannels and form fewer active sites. This is further evidenced by the high surface area (594 m²/g) exhibited by the catalyst (Table 1). However, as we moved from

Ag/SBA-15 to Ag/AP-SBA-15(O), conversion and selectivity was found to be significantly improved. This can be attributed to the fact that in one pot synthesis, that Ag NPs were implanted in the SiO₂ frameworks[16]. Moreover, as shown in the TEM image (Fig.4b) some of the Ag NPs also exist near the pore entrances (possibly due to the slight rupturing of the pore channels during metal incorporation) thus blocking the mesopores. Due to the blocking of

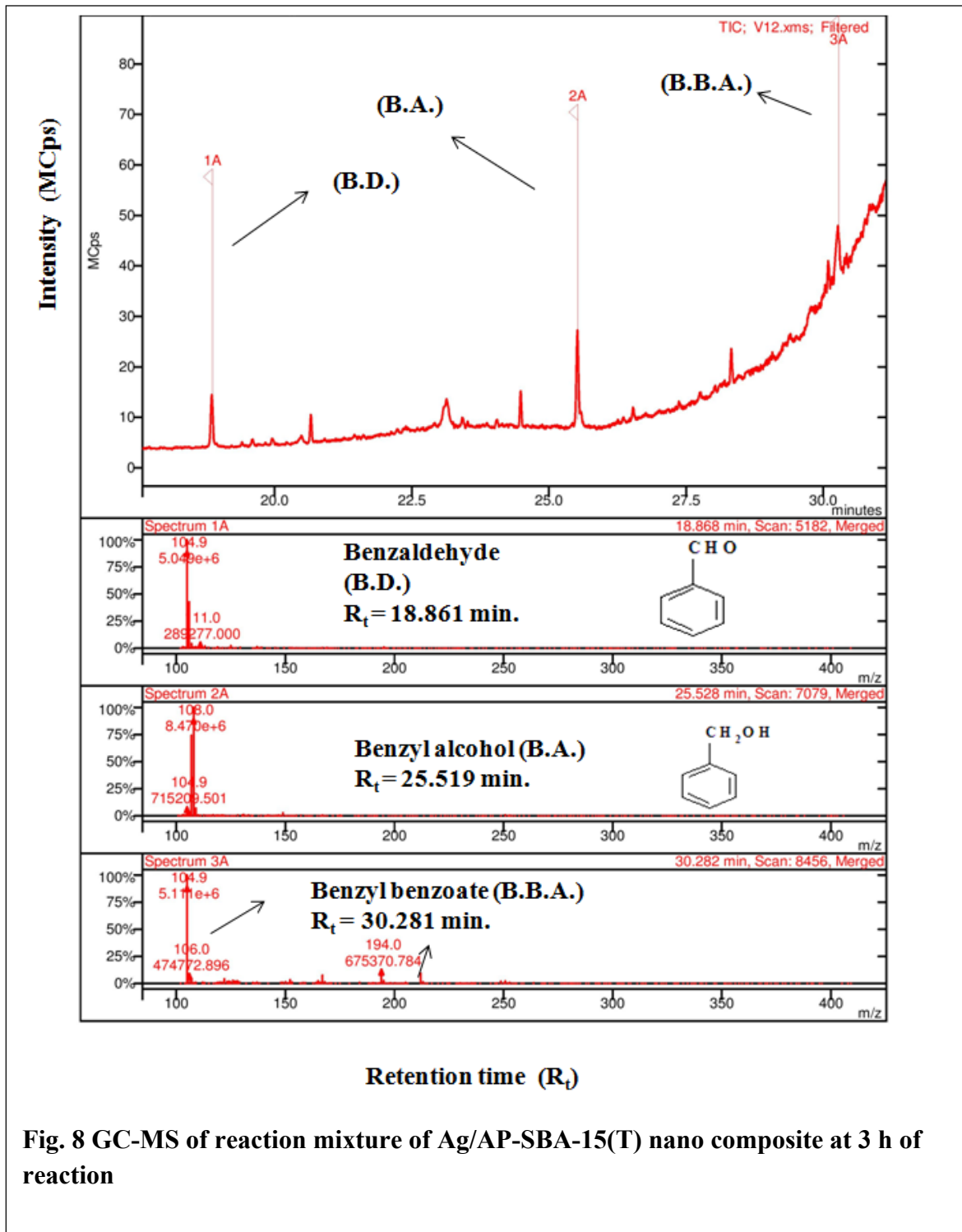


Fig. 8 GC-MS of reaction mixture of Ag/AP-SBA-15(T) nano composite at 3 h of reaction

some of the mesopores, fewer active sites were available for reaction, consequently leading to lower activity of Ag/AP-SBA-15(O) nanocomposites.

Moreover, to validate the stability of the Ag/AP-SBA-15(T) catalyst, reusability studies were done by filtering the catalyst followed by washing with ethanol and water. The catalyst was then dried overnight at 60 °C and used for the oxidation of benzyl alcohol. The catalyst exhibited high reusability for three recycles with a slight decrease in selectivity from 86 % to 78 % respectively.

6. Conclusion

In the present work, different Ag loaded SBA-15; nanocomposites were prepared by both in-situ direct synthesis as well as post-modified method for the selective oxidation of benzyl alcohol to benzaldehyde. Moreover, the effective role played by the surface functionalizing agent was also analyzed. It was concluded that the composites prepared by post-modified method showed the highest catalytic activity owing to the formation of comparatively smaller Ag nano particles (~8-10 nm) which were found to be uniformly distributed throughout the mesoporous matrix. Keeping in view the high catalytic efficiency exhibited by nanocomposites prepared by two-pot method, this method can also be extended to the formation of other mesoporous composites using other different transition metals for different redox reactions.

References

- [1] P. Kuhn, A. Forget, D. Su, A. Thomas, M. Antonietti, From microporous regular frameworks to mesoporous materials with ultrahigh surface area: dynamic reorganization of porous polymer networks, *Journal of the American Chemical Society*, 130 (2008) 13333-13337.
- [2] Y. Xia, R. Mokaya, A study of the behaviour of mesoporous silicas in OH/CTABr/H₂O systems: phase dependent stabilisation, dissolution or semi-pseudomorphic transformation, *Journal of Materials Chemistry*, 13 (2003) 3112-3121.
- [3] Q. Lu, F. Gao, S. Komarneni, T.E. Mallouk, Ordered SBA-15 nanorod arrays inside a porous alumina membrane, *Journal of the American Chemical Society*, 126 (2004) 8650-8651.
- [4] C. Kresge, M. Leonowicz, W. Roth, J. Vartuli, J. Beck, Ordered mesoporous molecular sieves synthesized by a liquid-crystal template mechanism, *nature*, 359 (1992) 710-712.
- [5] D. Zhao, Q. Huo, J. Feng, B.F. Chmelka, G.D. Stucky, Nonionic triblock and star diblock copolymer and oligomeric surfactant syntheses of highly ordered, hydrothermally stable, mesoporous silica structures, *Journal of the American Chemical Society*, 120 (1998) 6024-6036.
- [6] Y. Wang, X. Wang, Z. Su, Q. Guo, Q. Tang, Q. Zhang, H. Wan, SBA-15-supported iron phosphate catalyst for partial oxidation of methane to formaldehyde, *Catalysis today*, 93 (2004) 155-161.
- [7] D.V. Quang, P.B. Sarawade, A. Hilonga, S.D. Park, J.-K. Kim, H.T. Kim, Facile route for preparation of silver nanoparticle-coated precipitated silica, *Applied Surface Science*, 257 (2011) 4250-4256.
- [8] K. Chakrabarti, C. Whang, Silver doped or mosil—an investigation on structural and physical properties, *Materials Science and Engineering: B*, 88 (2002) 26-34.
- [9] C.M. Maroneze, L.P. da Costa, F.A. Sigoli, Y. Gushikem, I.O. Mazali, One-step preparation of silver nanoparticles confined in functionalized-free SBA-15 channels, *Synthetic Metals*, 160 (2010) 2099-2103.
- [10] S. Ramnani, S. Sabharwal, J.V. Kumar, K.H.P. Reddy, K.R. Rao, P.S. Prasad, Advantage of radiolysis over impregnation method for the synthesis of SiO₂ supported nano-Ag catalyst for direct decomposition of N₂O, *Catalysis Communications*, 9 (2008) 756-761.
- [11] W. Chen, J. Zhang, Y. Di, Z. Wang, Q. Fang, W. Cai, Size controlled Ag nanoparticles within pores of monolithic mesoporous silica by ultrasonic irradiation, *Applied Surface Science*, 211 (2003) 280-284.

- [12] J.-Y. Piquemal, G. Viau, P. Beaunier, F. Bozon-Verduraz, F. Fiévet, One-step construction of silver nanowires in hexagonal mesoporous silica using the polyol process, *Materials research bulletin*, 38 (2003) 389-394.
- [13] A. Keilbach, J. Moses, R. Köhn, M. Döblinger, T. Bein, Electrodeposition of copper and silver nanowires in hierarchical mesoporous silica/anodic alumina nanostructures, *Chemistry of materials*, 22 (2010) 5430-5436.
- [14] M. Imperor-Clerc, D. Bazin, M.-D. Appay, P. Beaunier, A. Davidson, Crystallization of β -MnO₂ nanowires in the pores of SBA-15 silicas: in situ investigation using synchrotron radiation, *Chemistry of materials*, 16 (2004) 1813-1821.
- [15] J. van der Meer, I. Bardez, F. Bart, P.-A. Albouy, G. Wallez, A. Davidson, Dispersion of Co₃O₄ nanoparticles within SBA-15 using alkane solvents, *Microporous and Mesoporous Materials*, 118 (2009) 183-188.
- [16] J. Han, P. Fang, W. Jiang, L. Li, R. Guo, Ag-nanoparticle-loaded mesoporous silica: spontaneous formation of Ag nanoparticles and mesoporous silica SBA-15 by a one-pot strategy and their catalytic applications, *Langmuir*, 28 (2012) 4768-4775.
- [17] I. Alonso-Lemus, Y. Verde-Gomez, A. Aguilar-Elguézabal, L. Álvarez-Contreras, Metal nanoparticles supported on Al-MCM-41 via in situ aqueous synthesis, *Journal of Nanomaterials*, 2010 (2010) 19.
- [18] H. Cui, Y. Zhang, L. Zhao, Y. Zhu, Adsorption synthesized cobalt-containing mesoporous silica SBA-15 as highly active catalysts for epoxidation of styrene with molecular oxygen, *Catalysis Communications*, 12 (2011) 417-420.
- [19] D. Tian, G. Yong, Y. Dai, X. Yan, S. Liu, CO oxidation catalyzed by Ag/SBA-15 catalysts prepared via in situ reduction: the influence of reducing agents, *Catalysis letters*, 130 (2009) 211-216.
- [20] K. Anisia, A. Kumar, Oxidation of cyclohexane with molecular oxygen using heterogeneous silica gel catalyst bonded with [1, 2-bis (salicylidene amino)-phenylene] zirconium complex, *Applied Catalysis A: General*, 273 (2004) 193-200.
- [21] S. Sareen, V. Mutreja, S. Singh, B. Pal, Highly dispersed Au, Ag and Cu nanoparticles in mesoporous SBA-15 for highly selective catalytic reduction of nitroaromatics, *RSC Advances*, 5 (2015) 184-190.

- [22] D. Margolese, J. Melero, S. Christiansen, B. Chmelka, G. Stucky, Direct syntheses of ordered SBA-15 mesoporous silica containing sulfonic acid groups, *Chemistry of materials*, 12 (2000) 2448-2459.
- [23] C.S. Chen, Y.T. Lai, T.W. Lai, J.H. Wu, C.H. Chen, J.F. Lee, H.M. Kao, Formation of Cu Nanoparticles in SBA-15 Functionalized with Carboxylic Acid Groups and Their Application in the Water–Gas Shift Reaction, *ACS Catalysis*, 3 (2013) 667-677.
- [24] X. Huang, M. Yang, G. Wang, X. Zhang, Effect of surface properties of SBA-15 on confined Ag nanomaterials via double solvent technique, *Microporous and Mesoporous Materials*, 144 (2011) 171-175.
- [25] R. Chimentao, I. Kirm, F. Medina, X. Rodriguez, Y. Cesteros, P. Salagre, J. Sueiras, J. Fierro, Sensitivity of styrene oxidation reaction to the catalyst structure of silver nanoparticles, *Applied Surface Science*, 252 (2005) 793-800.
- [26] X. Zhang, Z. Qu, F. Yu, Y. Wang, High-temperature diffusion induced high activity of SBA-15 supported Ag particles for low temperature CO oxidation at room temperature, *Journal of Catalysis*, 297 (2013) 264-271.
- [27] D.-H. Lin, Y.-X. Jiang, Y. Wang, S.-G. Sun, Silver nanoparticles confined in SBA-15 mesoporous silica and the application as a sensor for detecting hydrogen peroxide, *Journal of Nanomaterials*, 2008 (2008) 12.
- [28] K. Fuku, R. Hayashi, T. Kamegawa, K. Mori, H. Yamashita, Catalytic enhancement using localized surface plasmon resonance of color-controlled Ag nanoparticles deposited on mesoporous silica under microwave.
- [29] Y. Zhu, K. Morisato, W. Li, K. Kanamori, K. Nakanishi, Synthesis of silver nanoparticles confined in hierarchically porous monolithic silica: a new function in aromatic hydrocarbon separations, *ACS applied materials & interfaces*, 5 (2013) 2118-2125.
- [30] Á. Szegedi, M. Popova, J. Valyon, A. Guarnaccio, A. De Stefanis, A. De Bonis, S. Orlando, M. Sansone, R. Teghil, A. Santagata, Comparison of silver nanoparticles confined in nanoporous silica prepared by chemical synthesis and by ultra-short pulsed laser ablation in liquid, *Applied Physics A*, 117 (2014) 55-62.
- [31] A. Corma, From microporous to mesoporous molecular sieve materials and their use in catalysis, *Chemical reviews*, 97 (1997) 2373-2420.

- [32] Q. Huo, D.I. Margolese, P. Feng, T. Gier, P. Sieger, Generalized syntheses of periodic surfactant/inorganic composite materials, in, DTIC Document, 1994.
- [33] P.T. Tanev, T.J. Pinnavaia, Biomimetic templating of porous lamellar silicas by vesicular surfactant assemblies, *Science*, 271 (1996) 1267.
- [34] A.R. Hajipour, H. Karimi, A. Koohi, Selective oxidation of alcohols over nickel zirconium phosphate, *Chinese Journal of Catalysis*, 36 (2015) 1109-1116.
- [35] M. Tao, X. Meng, Y. Lv, Z. Bian, Z. Xin, Effect of impregnation solvent on Ni dispersion and catalytic properties of Ni/SBA-15 for CO methanation reaction, *Fuel*, 165 (2016) 289-297.
- [36] C. Rudolf, I. Mazilu, A. Chiriac, B. Dragoi, F. Abi-Ghaida, A. Ungureanu, A. Mehdi, E. Dumitriu, Copper nanoparticles supported on polyether- functionalized mesoporous silica. synthesis and application as hydrogenation catalysts, *Environmental Engineering and Management Journal*, 14 (2015) 399-408.
- [37] C.-H. Tu, A.-Q. Wang, M.-Y. Zheng, X.-D. Wang, T. Zhang, Factors influencing the catalytic activity of SBA-15-supported copper nanoparticles in CO oxidation, *Applied Catalysis A: General*, 297 (2006) 40-47.
- [38] M. Vinoba, S.-K. Jeong, M. Bhagiyalakshmi, M. Alagar, Electrocatalytic reduction of hydrogen peroxide on silver nanoparticles stabilized by amine grafted mesoporous SBA-15, *Bulletin of the Korean Chemical Society*, 31 (2010) 3668-3674.
- [39] G. Du, S. Lim, M. Pinault, C. Wang, F. Fang, L. Pfefferle, G.L. Haller, Synthesis, characterization, and catalytic performance of highly dispersed vanadium grafted SBA-15 catalyst, *Journal of Catalysis*, 253 (2008) 74-90.
- [40] C.Y. Ma, B.J. Dou, J.J. Li, J. Cheng, Q. Hu, Z.P. Hao, S.Z. Qiao, Catalytic oxidation of benzyl alcohol on Au or Au–Pd nanoparticles confined in mesoporous silica, *Applied Catalysis B: Environmental*, 92 (2009) 202-208.
- [41] A. Abad, P. Concepción, A. Corma, H. García, A collaborative effect between gold and a support induces the selective oxidation of alcohols, *Angewandte Chemie International Edition*, 44 (2005) 4066-4069.
- [42] M. Vazylyev, D. Sloboda-Rozner, A. Haimov, G. Maayan, R. Neumann, Strategies for oxidation catalyzed by polyoxometalates at the interface of homogeneous and heterogeneous catalysis, *Topics in Catalysis*, 34 (2005) 93-99.

- [43] C.-J. Li, G.-R. Xu, B. Zhang, J.R. Gong, High selectivity in visible-light-driven partial photocatalytic oxidation of benzyl alcohol into benzaldehyde over single-crystalline rutile TiO₂ nanorods, *Applied Catalysis B: Environmental*, 115 (2012) 201-208.
- [44] V. Choudhary, D. Dumbre, B. Uphade, V. Narkhede, Solvent-free oxidation of benzyl alcohol to benzaldehyde by tert-butyl hydroperoxide using transition metal containing layered double hydroxides and/or mixed hydroxides, *Journal of Molecular Catalysis A: Chemical*, 215 (2004) 129-135.
- [45] R. Mistri, D. Das, J. Llorca, M. Dominguez, T.K. Mandal, P. Mohanty, B.C. Ray, A. Gayen, Selective liquid phase benzyl alcohol oxidation over Cu-loaded LaFeO₃ perovskite, *RSC Advances*, 6 (2016) 4469-4477.
- [46] G.C. Behera, K. Parida, Liquid phase catalytic oxidation of benzyl alcohol to benzaldehyde over vanadium phosphate catalyst, *Applied Catalysis A: General*, 413 (2012) 245-253.
- [47] F.M. Menger, C. Lee, Synthetically useful oxidations at solid sodium permanganate surfaces, *Tetrahedron Letters*, 22 (1981) 1655-1656.
- [48] S. Alabbad, S. Adil, M. Assal, M. Khan, A. Alwarthan, M.R.H. Siddiqui, Gold & silver nanoparticles supported on manganese oxide: Synthesis, characterization and catalytic studies for selective oxidation of benzyl alcohol, *Arabian Journal of Chemistry*, 7 (2014) 1192-1198.
- [49] L. Geng, X. Zhang, W. Zhang, M. Jia, G. Liu, Highly dispersed iron oxides on mesoporous carbon for selective oxidation of benzyl alcohol with molecular oxygen, *Chemical Communications*, 50 (2014) 2965-2967.
- [50] F. Adam, W.-T. Ooi, Selective oxidation of benzyl alcohol to benzaldehyde over Co-metalloporphyrin supported on silica nanoparticles, *Applied Catalysis A: General*, 445 (2012) 252-260.
- [51] A. Jia, L.-L. Lou, C. Zhang, Y. Zhang, S. Liu, Selective oxidation of benzyl alcohol to benzaldehyde with hydrogen peroxide over alkali-treated ZSM-5 zeolite catalysts, *Journal of Molecular Catalysis A: Chemical*, 306 (2009) 123-129.
- [52] W. Zhu, Y. Han, L. An, Silver nanoparticles synthesized from mesoporous Ag/SBA-15 composites, *Microporous and Mesoporous Materials*, 80 (2005) 221-226.
- [53] X. Huang, W. Dong, G. Wang, M. Yang, L. Tan, Y. Feng, X. Zhang, Synthesis of confined Ag nanowires within mesoporous silica via double solvent technique and their catalytic properties, *Journal of colloid and interface science*, 359 (2011) 40-46.

- [54] A. Yin, C. Wen, W.-L. Dai, K. Fan, Ag/MCM-41 as a highly efficient mesostructured catalyst for the chemoselective synthesis of methyl glycolate and ethylene glycol, *Applied Catalysis B: Environmental*, 108 (2011) 90-99.
- [55] H. Chaudhuri, S. Dash, A. Sarkar, SBA-15 functionalised with high loading of amino or carboxylate groups as selective adsorbent for enhanced removal of toxic dyes from aqueous solution, *New Journal of Chemistry*, 40 (2016) 3622-3634.
- [56] M. Lombardo, M. Videla, A. Calvo, F. Requejo, G. Soler-Illia, Aminopropyl-modified mesoporous silica SBA-15 as recovery agents of Cu (II)-sulfate solutions: adsorption efficiency, functional stability and reusability aspects, *Journal of hazardous materials*, 223 (2012) 53-62.
- [57] V. Hernández-Morales, R. Nava, Y. Acosta-Silva, S. Macías-Sánchez, J. Pérez-Bueno, B. Pawelec, Adsorption of lead (II) on SBA-15 mesoporous molecular sieve functionalized with NH₂ groups, *Microporous and Mesoporous Materials*, 160 (2012) 133-142.
- [58] V. Subbaramaiah, V.C. Srivastava, I.D. Mall, Optimization of reaction parameters and kinetic modeling of catalytic wet peroxidation of picoline by Cu/SBA-15, *Industrial & Engineering Chemistry Research*, 52 (2013) 9021-9029.
- [59] X. Zhao, G. Lu, A. Whittaker, G. Millar, H. Zhu, Comprehensive study of surface chemistry of MCM-41 using ²⁹Si CP/MAS NMR, FTIR, pyridine-TPD, and TGA, *The Journal of Physical Chemistry B*, 101 (1997) 6525-6531.
- [60] N.N. Fathima, R. Aravindhan, J.R. Rao, B.U. Nair, Dye house wastewater treatment through advanced oxidation process using Cu-exchanged Y zeolite: A heterogeneous catalytic approach, *Chemosphere*, 70 (2008) 1146-1151.
- [61] L. Cheng, T. Rong, Y. Donghong, Y. Ningya, Z. Yuxu, Selective Oxidation of Benzyl Alcohol Catalyzed by Pd/PMO-SBA-15 Catalyst, *Chinese Journal of Catalysis*, 31 (2010) 1369-1373.

